VIP236: A small molecule drug conjugate with an optimized camptothecin payload has significant activity in patient-derived and metastatic cancer models

#484

DO NOT POST

B. Stelte-Ludwig[1], M.M. Frigault[2], H.G. Lerchen[1], T. Schomber[1], A.J Johnson[2], R. Izumi[2], A. Hamdy[2]

[1]Vincerx Pharma GmbH, Monheim, Germany; [2]Vincerx Pharma Inc., Palo Alto, CA, USA;

INTRODUCTION

VIP236 is a small molecule drug conjugate comprised of an $\alpha_v\beta_3$ integrin targeting moiety linked to an optimized camptothecin (optCPT) payload with a neutrophil elastase (NE) cleavable linker. $\alpha_v\beta_3$ has been used as target for anti-angiogenic treatments and is under clinical investigation with a good safety record. With VIP236 the targeting of activated $\alpha_v\beta_3$ allows for potent homing to the tumor microenvironment (TME) of most advanced and metastatic solid tumors, where the enriched NE cleaves the linker extracellularly and releases the optimized camptothecin payload. The payload is designed for rapid and efficient uptake into the tumor cell, while at the same time addressing the transporter liabilities of the camptothecin payload class resulting in a low efflux ratio. In the cell, the optCPT payload binds and inhibits DNA topoisomerase 1 (TOP1), leading to DNA damage and apoptosis.

We have previously shown that the high cytotoxic potency of VIP236 in vitro depends on NE cleavage, and a high potency of VIP236 in several CDX models was achieved[1,2]. Here we demonstrate the efficacy in patient-derived tumor PDX models and further evaluate of the mode of action.

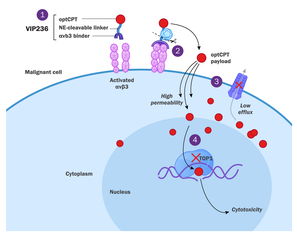

Figure 1. Mode of Action of VIP236.
(1) VIP236 is an $\alpha_v\beta_3$ integrin binder linked to an optCPT payload
(2) Neutrophil elastase (NE) in the tumor microenvironment specifically cleaves the linker releasing the payload
(3) OptCPT efficiently penetrates the cell membrane and accumulates in the tumor cell due to low efflux and resistance to drug transporters.
(4) The payload then inhibits topoisomerase 1 causing DNA damage and leading to cytotoxicity

METHODS

- Lung (LXFL 529) and renal (RXF 2667) PDX models comprised six groups each with 10 animals. Tumor fragments (3-4 mm edge length) were transplanted, and tumor growth was monitored until a median size of about 120-150 mm³ was achieved. VIP236 was administered at 20/30/40 and 60 mg/kg intravenously over the course of 38 days. Therapy was supplied in a 3 days on/4 days off (control, 20/40 mg/kg) or 2 days on/5 days off (30/40 mg/kg) dosing schedule as well as once weekly (60 mg/kg). Both experiments were terminated after a three-week observation phase on day 63. Animals were routinely monitored at least twice daily on working days and at least once daily on weekends (tumor size and body weight measurement).
- Colon (CXF2068) and TNBC (MAXF BR 120) PDX models were performed as describe above with changes in schedule. VIP236 was administered at 20 mg/kg (group 3), 40 mg/kg (group 2 and group 5) and 60 mg/kg (group 4). Therapy was supplied in a 2 days on 5 days off schedule in groups 2 and 3 or once weekly in group 4. Therapy in group 5 followed a 2 days on 12 days off pattern. Statistical significance of antitumor efficacy was analyzed by the non-parametric Kruskal-Wallis test followed by Dunn's method for multiple comparisons using GraphPad Prism bioanalytic software (version 9.10) with p<0.05 as significant. Additionally, an unpaired t-test was performed using GraphPad Prism (version 9.10).
- Orthotopic TNBC model MA4296: Cells were inoculated into the mammary fat pad of mice. Treatment started on day 20, when palpable tumor sizes reached (127 mm³). VIP236 was administered via intravenous injection with 40 mg/kg of VIP236 at two successive days followed by 5 days off or with 60 mg/kg of VIP236 once weekly for 4 weeks. Tumors were measured twice weekly with calipers and their volume was calculated with the formula: (length x width²)/2. The body weight was determined two times weekly and recorded as individual data then calculated as median and mean body weight and body weight change in percent. All animals were monitored daily for treatment-related toxicity.
- IHC analysis: The tissues were examined according to standard protocol and in parallel evaluated for necrotic areas, connective tissue - the analysis was restricted to vital neoplastic cells. Semiquantitative IHC-scoring scale (- to +++) was related to percent staining of neoplastic cell (0%-100%) to deduce a composite score. Light microscopic images acquired at 200x magnification and evaluation of 10 high power fields were averaged)
- γH2Ax staining: Tumor samples were fixed in 10% Formalin for 24h. FFPE samples were sectioned at 3 µm and stained according to standard IHC protocol. Multiplexed analysis was performed with QuPath.
- PCR analysis: To detect human tumor cells, a human-specific RealTime DNA PCR using an optimized primer-probe assay targeting the alpha-satellite region of the human chromosome 17 was performed. DNA was isolated from liver, lung and brain of all mice per group. The PCR reaction and quantification is performed in a StepOnePlus™ RealTime PCR System (LightCycler 480 II system (Hoffmann-La Roche) applying the standard protocol supplied by the manufacturer. For semi-quantitative evaluation the Cp value is used. Statistical analysis was performed using unpaired t-test.

RESULTS

Verifying $\alpha_v\beta_3$ and Neutrophil Elastase Presence in Patient Samples and Confirming Induced DNA Damage

Patient samples (≥50 each indication) were evaluated to confirm $\alpha_v\beta_3$ and neutrophil elastase presence in advance cancers, where clinical data indicates correlation of NE expression and poor prognosis[3]. In some indications additional membranous staining of $\alpha_v\beta_3$ on the tumor cells was observed (e.g., renal). To confirm DNA damage conferred by VIP236-mediated TOP1 inhibition, tumors from the SNU16 CDX mouse model treated with VIP236 were stained for phosphorylated γH2Ax as a marker for DNA damage. A time-dependent γH2Ax phosphorylation was observed.

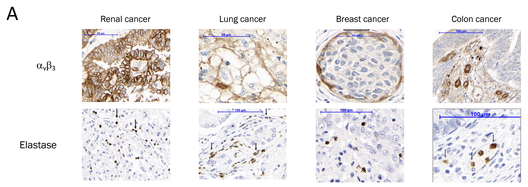

Figure 2. IHC analysis of relevant biomarker.
(A) Representative images of IHC analysis of $\alpha_v\beta_3$ and neutrophil elastase performed with at least 50 patient samples for each indication **(B)** Representative images of γH2Ax staining after one treatment cycle with VIP236 of SNU16 mouse xenograft samples

Monotherapy of VIP236 achieved Potent and Durable anti Tumor Activity in Patient-derived Tumor Mouse Models

The PDX models were selected based on indications with high unmet medical need and hard to treat cancers, like liver metastasis from a patient with colon cancer. All models show a good tolerability of VIP236. The regrowth-phases, post-treatment, demonstrate a long-lasting effect of anti-tumor efficacy in all models.

VIP236 achieved especially high efficacy in NSCLC with durable CR responses. Partial responses and stable diseases were obtained in colon cancer, renal cancer and TNBC depending on the treatment schedule.

Table 1. Patient characteristics of patient-derived material.

Cancer type	Patient histology	Gender/Age	Ethnicity	Primary/ Metastasis/ Recurrent	Site of origin	Mutation profile
Lung Cancer	NSCLC	Female / 34	Caucasian	Primary	Lung	TP53 - G244C; EGFR - T678R
Colorectal Cancer	adeno carcinoma	Male / 50	Caucasian	Metastasis	Liver	TP53 - mut KRAS - G12V
Renal Cancer	clear cell carcinoma	Female / 61	Caucasian	Not known	Kidney	TP53 wt KRAS wt
TN Breast Cancer	invasive ductal carcinoma	Female / 52	Caucasian	Primary	Breast	TP53 - low coverage
Gastric Cancer	adeno carcinoma	Male / 62	Asian	Primary	Stomach	TP53 - mut KRAS wt

A

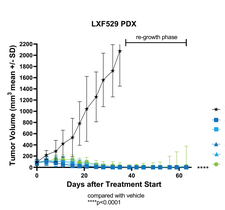

B

Dosing	CR	PR	SD	PD
Vehicle	-	-	-	7
40 mg/kg 3on/4off	8	2	-	-
20 mg/kg 3on/4off	5	5	-	-
40 mg/kg 2on/5off	3	7	-	-
30 mg/kg 2on/5off	6	4	-	-
60 mg/kg QW	2	7	1	-

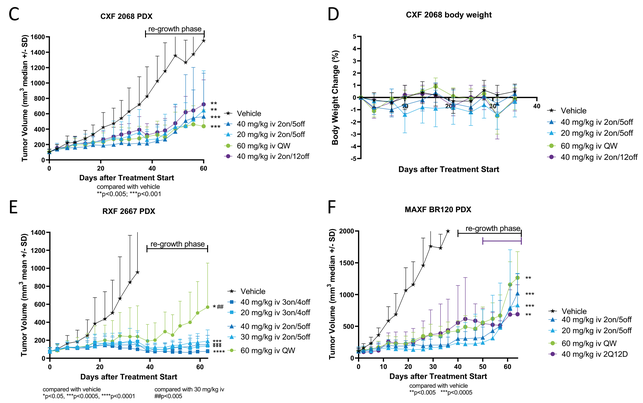

Figure 3. Different patient-derived mouse models treated successfully with VIP236 in monotherapy.
(A) Growth curves of patient-derived lung cancer LXF529 model. **(B)** Complete responses were achieved in most treatment groups. All schedules and doses tested exhibit statistical significance p<0.0001 vs vehicle **(C)** Growth curve of patient-derived colorectal cancer CXF 2068 model. Statistically significant tumor growth inhibition (p<0.001 vs vehicle, p<0.005 vs vehicle) was observed in this liver metastasis CRC PDX model with all schedules **(D)** Corresponding body weight changes indicate good tolerability of all doses **(E)** Growth curves of patient-derived renal cancer RXF 2667 model. Partial regression was observed with sustained antitumor activity in the 3on/4off and 2on/5off schedules compared with once weekly treatment (p<0.005). **(F)** Growth curve of patient-derived breast cancer MAXF BR120 model. Statistically significant tumor growth inhibition (p<0.005) was observed at all doses and schedules compared with vehicle.

Evaluation of Orthotopic Metastatic TNBC PDX Mouse Models

Due to $\alpha_v\beta_3$ upregulation during metastasis formation, we specifically investigated the effect of VIP236 in an orthotopic TNBC metastasis model. The metastatic TNBC PDX model MA4296 derived from a relapsed/refractory patient was successfully treated with VIP236 achieving significant regression of the primary tumor (Fig 4A). In lung and brain tissue, a significant reduction of metastases was detected. In liver the effect of metastasis reduction was reduced, however here metastasis formation was lower than in brain and lung (Fig 4B). Importantly IHC analysis reveals an increased $\alpha_v\beta_3$ and NE staining as consequence of treatment, while TOP1 staining was stable (Fig 4C,4D).

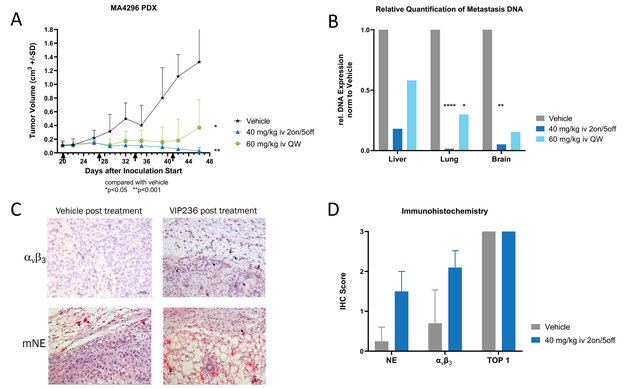

Figure 4. Significant impact of VIP236 on primary tumor and metastases in metastatic TNBC mouse model.
(A) Growth curves of metastatic TNBC MA4296 PDX model. Regression is observed in the 40 mg/kg 2on/5off treatment group (p<0.001 vs vehicle). **(B)** Relative quantification of metastases DNA exhibit significant reduction of metastases in lung which was achieved with both schedules (***p<0.0001 for 40 mg/kg 2on/5 off and *p<0.05 for 60 mg/kg QW vs vehicle). In brain tissue significant reduction of metastasis formation was observed for the 2on/5off schedule (**p<0.01 vs vehicle). **(C)** Representative IHC images exhibit increase in $\alpha_v\beta_3$ and NE. **(D)** Median of IHC scores displayed comparing vehicle with treated group (n= 10 animals.) Statistical significance was analyzed by unpaired t-test.

High Potency in HER2^{low} Gastric Cancer PDX Mouse Models showing independence of HER2 Status

VIP236 treatment resulted in statistically significant tumor growth inhibition in gastric PDX and CDX cancer models independent of HER2 status (NCI H87 HER2^{high} data not shown and SNU16 HER2^{neg}).

A HER2^{low} expressing patient-derived mouse model was selected to evaluate the efficacy of VIP236 monotherapy. An anti-HER2 ADC (fam-trastuzumab deruxtecan) was used as a comparator, as the payload is also a TOP1 inhibitor.

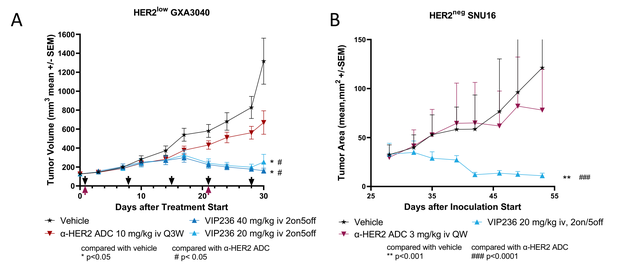

Figure 5. VIP236 efficacy in HER2^{low} gastric cancer models.
(A) Growth curves of patient-derived gastric cancer HER2^{low} GXA3040 model. VIP236 shows a statistically significant reduction in tumor growth compared to vehicle or α-HER2 ADC. α-HER2 ADC itself shows limited tumor growth inhibition. **(B)** Growth curves in HER2^{neg} SNU16 CDX gastric cancer model. VIP236 demonstrates significant tumor growth inhibition. α-HER2 ADC demonstrates no anti-tumor activity in the HER2^{neg} model

CONCLUSIONS

- In patient samples NE staining as well as $\alpha_v\beta_3$ staining on endothelial cells and in some indications also on tumor cells could be confirmed, further underlining the potential of VIP236 as a pan-solid tumor agent in advanced and metastatic cancers.
- Treatment dependent phosphorylation of γH2Ax, as marker for DNA damage, verifies the on-target activity of the liberated optCPT payload derived from VIP236.
- VIP236 monotherapy exhibits high potency in a broad panel of patient-derived mouse models with excellent tolerability. After treatment termination, a long duration of tumor growth inhibition is observed.
- In the orthotopic metastatic breast cancer PDX model IHC analysis reveals an increase of $\alpha_v\beta_3$ and NE staining due to VIP236 treatment while TOP1 expression is stable. This could be a possible explanation for the durable anti-tumor efficacy (a positive feedback loop) and helps explain the no to slow regrowth of the tumor after the end of treatment.
- Metastases formation is successfully reduced in lung tissue, but also in hard to target brain metastases a significant reduction is measured. This observation could indicate blood brain barrier penetration of VIP236.
- Superiority to fam-trastuzumab deruxtecan and independence of HER2 expression of VIP236 is shown in a gastric PDX model and CDX models.
- VIP236 is being evaluated in a first-in-human study in subjects with advanced or metastatic solid tumors (NCT05712889).

REFERENCES

1. Lerchen H.-G. Stelte-Ludwig B., et al, Cancers 2022
2. AACR 2021 Abstract #1314
3. Sato T, Takahashi S, Mizumoto T, et al, Surgical Oncol. 2006

ACKNOWLEDGMENTS

Special thanks to Charles River Laboratories Germany GmbH and epo-GmbH who performed the in vivo PDX studies, PCR analysis and IHC analysis. We thank provitro AG Germany for performing IHC analysis on patient samples and Nuvisan for IHC analysis of tumor samples.

Corresponding author: B. Stelte-Ludwig (Beatrix.Stelte-Ludwig@Vincerx.com)

Presented at the AACR ANNUAL MEETING 2023, April 14-19, 2023, Orlando, Florida